

# Experimental measurements of flow and sediment transport through bottom racks. Influence of gravel sizes on the rack

Luis G. Castillo, Juan T. García & José M. Carrillo

*Civil Engineering Department, Hidr@m I+D+i Group, Universidad Politécnica de Cartagena, Spain*

**ABSTRACT:** This work is focused on the study of bottom rack intake systems for discontinuous and torrential streams. The cases of clear water and water with gravel sediments have been analyzed. Different tests have been carried out to quantify the influence of the solids passing through the racks. Results of the wetted rack lengths and efficiency of racks are presented. The clear water cases have been modeled with computational fluid dynamics, and compared with the measured obtained in Universidad Politécnica de Cartagena. Experimental and numerical studies that characterize both, the clear water and the influence of solid load in the operation of the bottom racks, will allow to improve the existing design criteria.

## 1 INTRODUCTION

Bottom rack intake systems are designed to get the maximum quantity of water in mountain rivers with important transport of sediments. Orth et al. (1954) studied the efficiency of some bars shapes to capture the most quantity of water. Ract-Madoux et al. (1955) presented their experiences in several intake systems located in French Alps (Fig. 1). They described the influence of the sediment load in the racks obstruction. They also analyzed how to remove the incoming sediments.

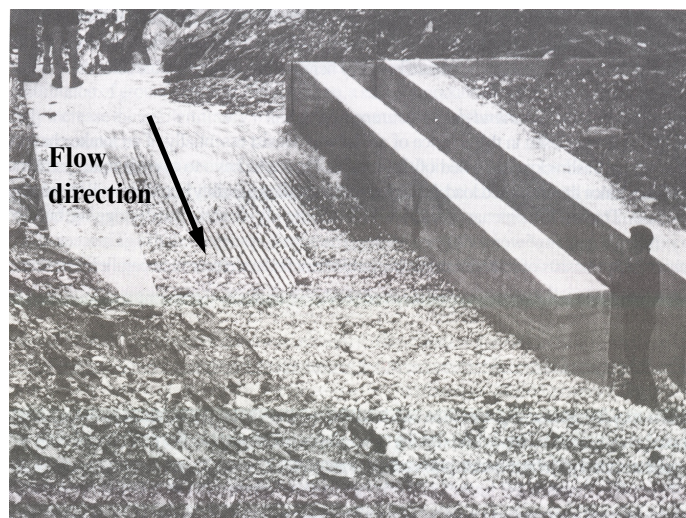


Figure 1. Gravels size materials occlude the bottom rack intake system (Ract-Madoux et al. 1955).

Drobir (1981) and Bouvard (1992) also proposed some criteria for the construction of intake systems

based on the sieve curves of the existing sediments in continuum flow rivers. Different parameters such as the longitudinal slope of the rack, the bar clearance, or the shape of bars were selected depending on the characteristics of the solid load. Drobir (1999) carried out measurements in a prototype located in a torrential stream, and compared the results with the theoretical length for the case of a rack tested with clear water.

Taking into account previous results, experimental tests have been carried out in the Hydraulic Laboratory of the Universidad Politécnica de Cartagena (UPCT). The occlusion of bottom racks due to gravel size solids has been analyzed (Fig. 2).

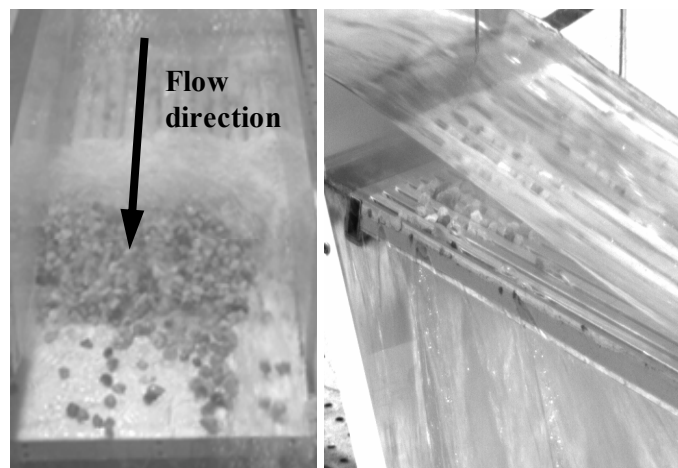


Figure 2. Rack partly occlude by the gravel transport (UPCT laboratory).

In the analysis of clear water flows, some simplifications are often assumed: the flux over the rack is one-dimensional, the flow decreases progressively,

the hydrostatic pressure distribution acts over the rack in the flow direction, the energy level or energy head along the rack is considered constant.

Several researchers analyzed these simplifications by means of laboratory hydraulic models. Noseda (1956) studied the clear water flow through different racks. He defined for horizontal rack case and subcritical approximation flow a variable discharge coefficient:

$$C_q = 0.66m^{-0.16} \left( \frac{h}{l} \right)^{-0.13} \quad (1)$$

where  $l$  is referred to the inter axis (distance between the centerline of two consecutive bars),  $m$  is the void ratio, and  $h$  is the height of water measured in the vertical direction.

According to Brunella et al. 2003, differences between measured and calculated depth profiles are generally found at the beginning of the rack due to the consideration of hydrostatic pressure distribution, and at the end of the rack when wall friction effects are neglected.

Righetti & Lanzoni (2008) proposed to calculate the flow derived by the rack with the following differential equation:

$$dq(x) = C_q m \sqrt{2g(H_0 + \Delta z)} dx \quad (2)$$

where  $m$  is the void ratio,  $dx$  the differential rack length in the flow direction,  $H_0$  the total energy at the beginning of the rack,  $\Delta z$  the vertical distance between the edge of the rack and the analyzed section, and  $C_q$  the discharge coefficient. The same authors proposed that  $C_q \approx \sin \alpha$ , being  $\alpha$  the angle between the velocity vector of water derived and the plane of the rack.

Several researchers such as Frank (1956), Bouvard & Kuntzmann (1954) and Noseda (1956) estimated the theoretical wetted rack length  $L$  necessary to derive a defined flow rate (See Table 1).

Table 1. Formulations for flow profiles and wetted rack lengths.

Bouvard & Kuntzmann (1954)

$$L = \left\{ \frac{1}{2m'} \left[ \left( j + \frac{1}{2j^2} \right) \cdot \arcsin \sqrt{\frac{j}{j + (1/2j^2)}} \right. \right. \\ \left. \left. + 3 \sqrt{\frac{1}{2j}} \right] + \left( \frac{0.303}{m'^2} + \frac{2j^3}{4j^2} \frac{3j^2 + 1}{4j^2} \right) \cdot \text{tg} \varphi \cdot h_1 \right\} \cdot \cos \varphi \\ j = \frac{h_1}{h_c}; \quad m' = m \cdot C_q$$

where:  $h_1$  = depth at the beginning of the rack  
 $h_c$  = critical depth

Noseda (1956)

$$L = \frac{H_0}{C_q \cdot m} [\Phi(y_2) - \Phi(y_1)]; \quad \Phi = f(y); \quad y = \frac{h}{H} \\ L = 1.1848 \frac{H_0}{C_q \cdot m}$$

Frank (1956)

$$L = 2.561 \frac{q_1}{\lambda \sqrt{h_1}}; \quad \lambda = m C_{q_0} \sqrt{2 \cdot g \cdot \cos \varphi}; \\ C_{q_0} = 1.22 C_{q_{x=x_0}} \\ \text{where: } h_1 = \text{depth at the beginning of the rack} \\ q_1 = \text{incoming specific flow} \\ \varphi = \text{angle of the rack with the horizontal plane}$$

Krochin (1973)

$$L = \left[ \frac{0.313 q_1}{(C_q k)^{3/2}} \right]^{2/3}; \quad k = (1-f)m; \quad f = 0.15 - 0.30 \\ \text{where: } q_1 = \text{incoming specific flow} \\ f = \text{obstruction coefficient}$$

Castillo & Lima (2010) analyzed and compared the formulae of wetted rack length obtained by the researchers of Table 1 (Fig. 3).

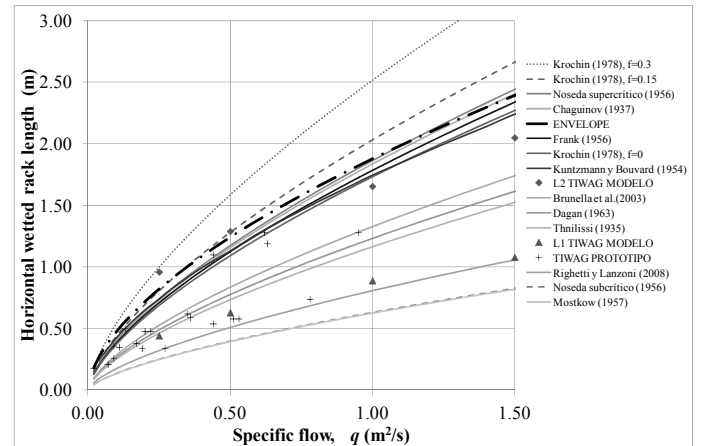


Figure 3. Lengths calculated with different formulae, and measured in reduced models and prototype, for flow between bars  $L_1$ , and flow over bars  $L_2$ . Case of circular bars with  $m = 0.6$  (Castillo & Lima 2010).

## 2 MATERIALS AND METHODS

### 2.1 Physical device

An intake system has been constructed in the Hydraulic Laboratory of the Universidad Politécnica de Cartagena (Fig. 4). It consists of a 5.00 m long and 0.50 m wide approximation channel, a rack with different slopes (from horizontal to 33%), a discharge channel and the channel to collect derived water.



Figure 4. Intake system physical device at Universidad Politécnica de Cartagena, Spain.

Three different racks, with 0.9 m length, are available. All of them are made of aluminum bars with  $T$  profiles (T 30/25/2 mm). Bars are disposed longitudinally to the inlet flow. The difference between the racks is the spacing between bars, so different void ratios are available. Table 3 summarizes the geometric characteristics of each rack.

Table 3. Geometric characteristic of racks.

Experiment	A	B	C
Spacing between bars, $b_1$ (mm)	5.70	8.50	11.70
Void ratio			
$m = \frac{b_1}{b_1 + 30}$	0.16	0.22	0.28

## 2.2 Clear water experimental tests

Test with clear water for the three racks A, B, and C have been done adopting different specific flows (53.8, 77.0, 114.6, 138.88, 155.4 l/s/m) and rack slopes (0%, 10%, 20%, 30%, 33%). The incoming flow,  $q_1$ , is measured in an electromagnetic flowmeter at the beginning of the channel. The rejected flow,  $q_2$ , is measured by using a V-notch weir placed in the channel that collects rejected flows. The flow derived by the rack,  $q_d$ , is calculated as a difference between  $q_1$  and  $q_2$ .

In each test, the flow depth along the rack was measured. According to Drobir (1999), the horizontal projection of the distance along the rack where the nappe crossed the axis of the rack (measured between the bars),  $L_1$ , and the maximum horizontal distance where the bars are wet,  $L_2$ , were also measured (Fig. 5).

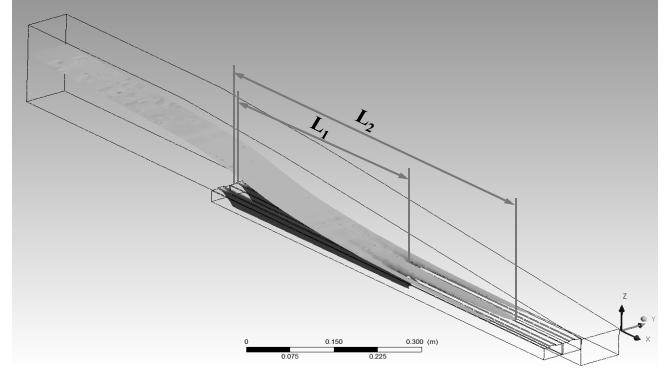


Figure 5. Scheme of wetted rack lengths  $L_1$  and  $L_2$ .

## 2.3 Clear water numerical simulations

To test the hydraulic compartment of the intake system, laboratory measurements were used to model and calibrate CFD programs. For the turbulent flow, CFD codes solve the differential Reynolds-Averaged Navier-Stokes (RANS) equations of the phenomenon in the fluid domain, retaining the reference quantity in the three directions for each control volume identified. The equations for conservation of mass and momentum may be written as:

$$\frac{\partial \rho}{\partial t} + \frac{\partial (\rho U_j)}{\partial x_j} = 0 \quad (3)$$

$$\frac{\partial \rho U_i}{\partial t} + \frac{\partial (\rho U_i U_j)}{\partial x_j} = -\frac{\partial p}{\partial x_i} + \frac{\partial}{\partial x_j} (2\mu S_{ij} - \overline{\rho u_i' u_j'}) \quad (4)$$

where  $i$  and  $j$  are indices,  $x_i$  represents the coordinate directions ( $i = 1$  to 3 for  $x$ ,  $y$ ,  $z$  directions, respectively),  $\rho$  the flow density,  $t$  the time,  $U$  the velocity vector,  $p$  the pressure,  $u_i'$  presents the turbulent velocity in each direction ( $i = 1$  to 3 for  $x$ ,  $y$ ,  $z$  directions, respectively),  $\mu$  is the molecular viscosity,  $S_{ij}$  is the mean strain-rate tensor and  $-\overline{\rho u_i' u_j'}$  is the Reynolds stress.

Eddy-viscosity turbulence models consider that such turbulence consists of small eddies which are continuously forming and dissipating, and in which the Reynolds stresses are assumed to be proportional to mean velocity gradients. The Reynolds stresses may be related to the mean velocity gradients and eddy viscosity by the gradient diffusion hypothesis:

$$-\overline{\rho u_i' u_j'} = \mu_t \left( \frac{\partial U_i}{\partial x_j} + \frac{\partial U_j}{\partial x_i} - \frac{2}{3} \delta_{ij} \rho k + \mu_t \frac{\partial U_k}{\partial x_k} \right) \quad (5)$$

with  $\mu_t$  being the eddy viscosity or turbulent viscosity,  $k = 1/2 \overline{u_i' u_i'}$  the turbulent kinetic energy and  $\delta$  the Kronecker delta function.

For the numerical modeling, the CFD volume finite scheme program ANSYS CFX (version 14.0) has been used. The  $k-\omega$  based Shear-stress-Transport (SST) turbulence model was selected to complement the numerical solution of the Reynolds-averaged Navier-Stokes equations (RANS). To solve the two-phase air-water, the homogeneous model was used.



the UPCT laboratory. Figures 9-10 show the longitudinal flow profiles for three specific flows (77.0, 114.6 and 155.4 l/s/m), and spacing  $b_l = 11.70$  mm ( $m = 0.28$ ) measured and simulated over a bar. The rack was horizontal in Figure 9, while it had and slope of 20 % in Figure 10.

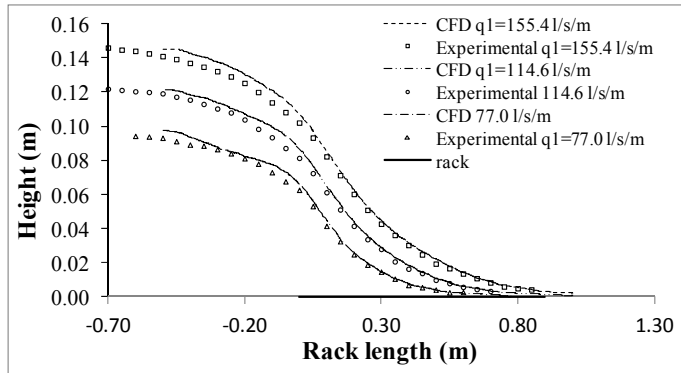


Figure 9. Flow profiles over a bar measured and modeled with CFD, for horizontal slope and considering rack C ( $m = 0.28$ ).

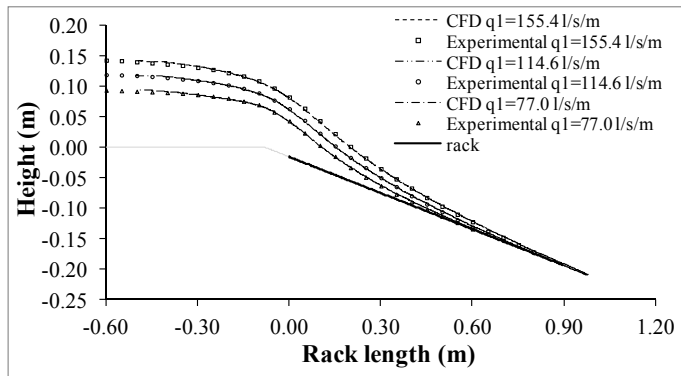


Figure 10. Flow profiles over a bar measured and modeled with CFD, for 20% slope and considering rack C ( $m = 0.28$ ).

In order to know the degree of accuracy, details of the water profiles at the end part of the rack appear in Figures 11-12.

In both cases, the values measured and calculated show a good agreement.

The length of the rack necessary to derive a determinate flow is an interesting design parameter. Hence, experimental measurements and CFD simulated values of  $L_1$ ,  $L_2$  have been used to compare the length value  $L$  calculated with different formulae.

As a result of the shape of the T bars, the surface tension phenomena tends to cause high values of  $L_2$ , even when more than 95% of  $q_l$  is derived in the vicinity of  $L_1$ . The length of wetted rack that ensures to capture almost all the incoming flow is near a water height of 3 mm. This point has been used to estimate the experimental length  $L$  at laboratory.

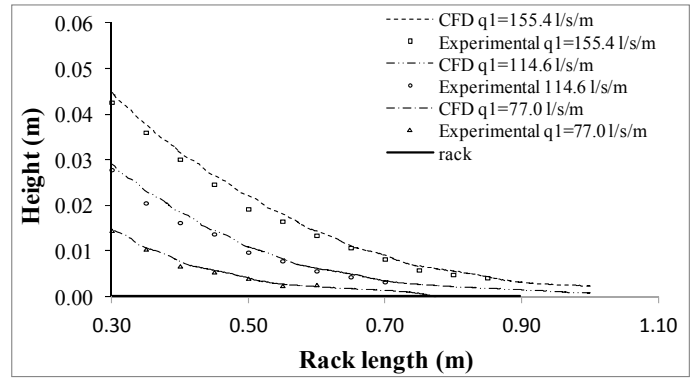


Figure 11. Detail of the flow profiles over a bar measured and modeled with CFD, for horizontal slope and considering rack C ( $m = 0.28$ ).

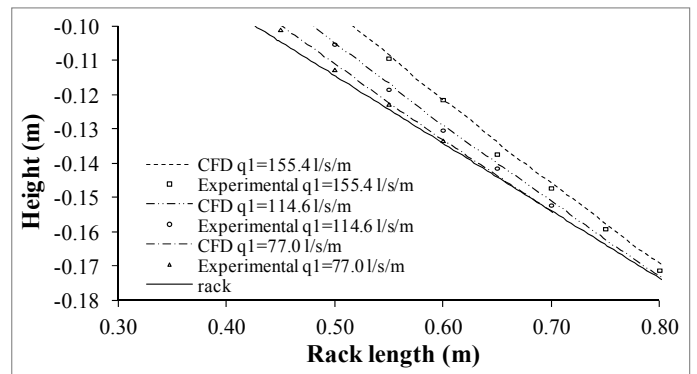


Figure 12. Detail of the flow profiles over a bar measured and modeled with CFD, for 20% slope and considering rack C ( $m = 0.28$ ).

Figures 13-14 show the results obtained with  $m = 0.28$ , and two different slopes. Some specific flows had lengths that exceeded the available length of the racks (0.90 m), so they could not been measured. A good agreement was obtained between the existing formulae, the CFD results and the experimental measurements.

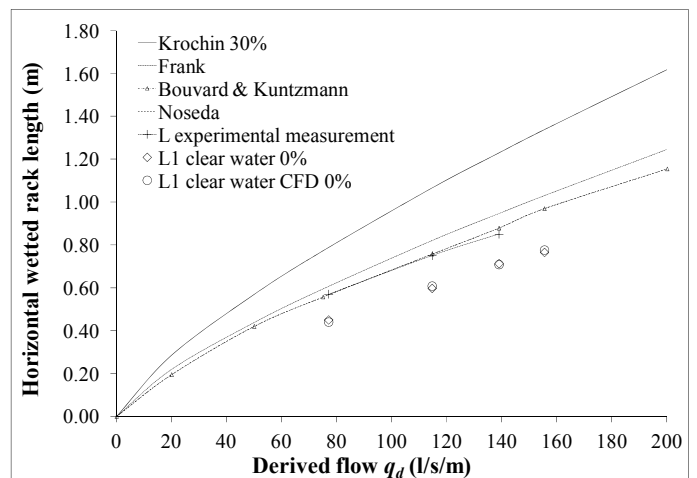


Figure 13. Wetted rack lengths (horizontal projection) for an horizontal rack C, with  $m = 0.28$ , and considering different flow rates.

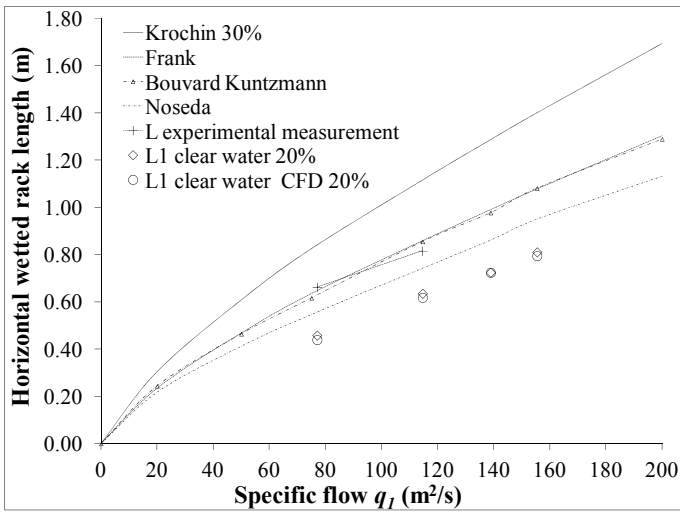


Figure 14. Wetted rack lengths (horizontal projection) for an 20% slope rack C, with  $m = 0.28$ , and considering different flow rates.

### 3.2 Test with gravels

Due to the deposition of part of the gravel into the spacing between bars, the flow depth along the rack increases (Fig. 15). Hence, the decrease in the void fraction drives to a reduction in the flow derived.

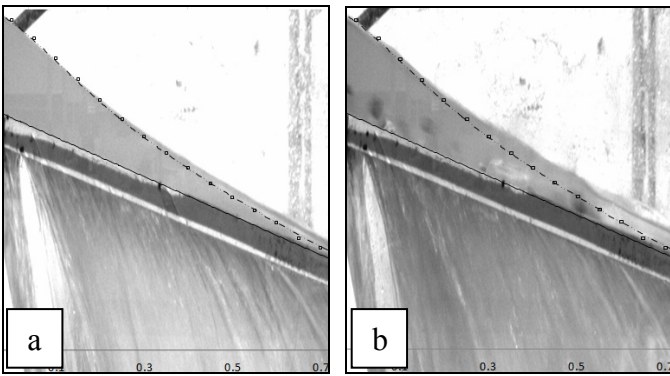


Figure 15. Water profile over the rack for rack C ( $m = 0.28$ ) 20% slope,  $q_1 = 155.4$  l/s/m. a) Clear water case; b) water with gravel 2 case.

The rejected flow,  $q_2$ , (the flow that is not collected by the intake system) varies during the tests series. Figures 16-17 show the evolution of the rejected flow along the test series for the rack C and two different flows (114.6 and 155.4 l/s/m). The bigger changes in the ratio of rejected flow occurs at the beginning of the test. In the final part, the flow not derived for the rack tends to a constant value.

The deposition/obstruction zones along the rack tends to occurs in the initial parts or the rack. Hence, the phenomenon has more influence in the parts where the higher angles between the velocity vector of water derived and the plane of the rack appears. This matches with the research carried out by several authors (Riguetti & Lanzoni 2008, Castillo & Carrillo 2012, Castillo et al. 2013).

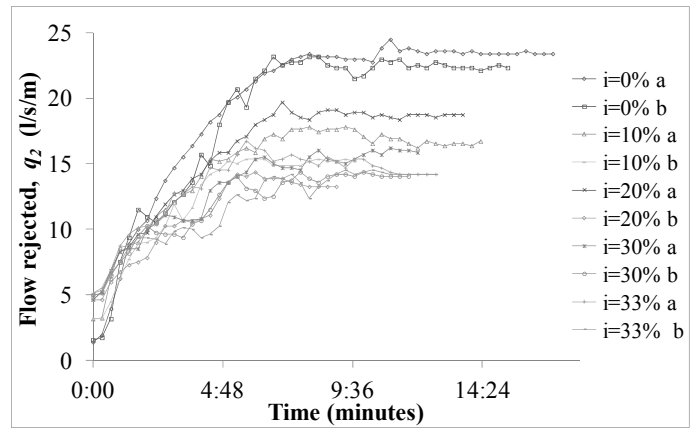


Figure 16. Time evolution of the rejected flow for tests carried out with the rack C ( $m = 0.28$ ), gravel 2, and  $q_1 = 155.4$ , when several slopes are considered.

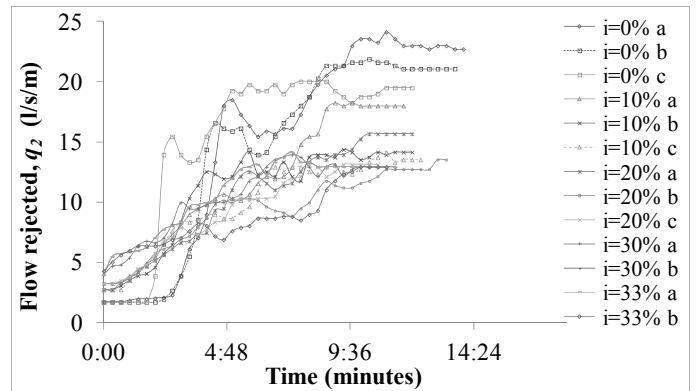


Figure 17. Time evolution of the rejected flow for tests carried out with the rack C ( $m = 0.28$ ), gravel 2, and  $q_1 = 114.5$ , when several slopes are considered.

For each test, the relations between the flow at the inlet,  $q_1$ , and the flow derived by the rack,  $q_d$ , appears in Figures 18-19 when the equilibrium was reached. The influence of the deposit of gravels between the bar reduce the void fraction. So, both figures show the reduction of the water derivation capacity from the clear water experiments.

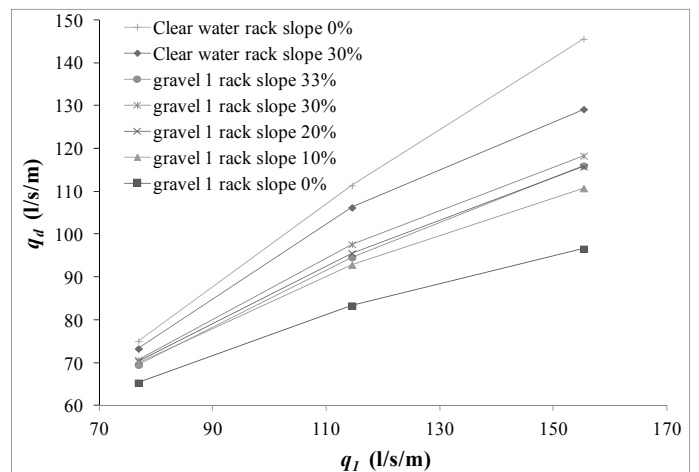


Figure 18. Derivation capacity for rack B ( $m = 0.22$ ) and gravel 1 in function of rack slope.

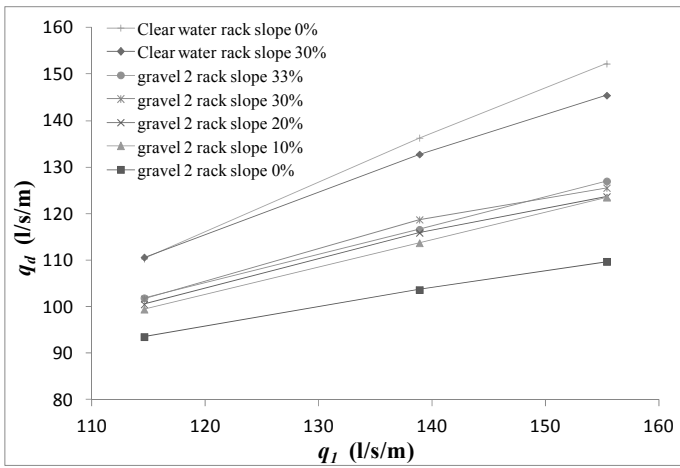


Figure 19. Derivation capacity for rack C,  $m = 0.28$ , and gravel 2 in function of rack slope.

The slope of the rack in the clear water experiments tends to reduce the collected water. In this way, when the rack B ( $m = 0.22$ ) is tested, the flow collected is reduced near 10% when the slope changes from 0 to 30%. However, when the rack C ( $m = 0.28$ ) is tested, the reduction is near 6%.

Considering the gravel cases, the maximum efficiency is obtained when the slope is 30%. The worst efficiency is obtained with the horizontal rack, with a maximum reduction of 33% for the rack B and 29% for the rack C.

The wetted rack length  $L_l$  has been also measured for each test. Figures 20-21 represents the length  $L_l$  measured with racks B and C. Tests carried out with the same incoming flow show a tendency to reduce the derived flow and to increase of  $L_l$  with the different slopes. The general behavior is the increase of those lengths due to the gravels deposited between the bars. In most cases,  $L_l$  reached the length of the tested rack (0.90 m). This is caused by the reduction of the derived flow.

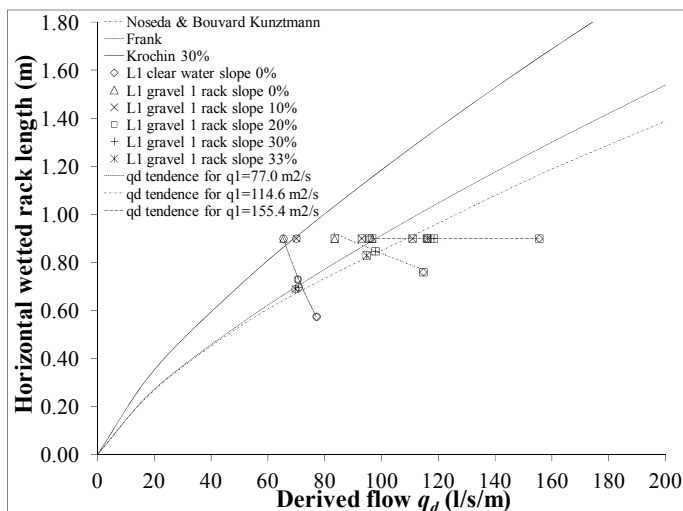


Figure 20. Wetted rack lengths (horizontal projection) for tests carried out with gravel 1, rack B and different flows.

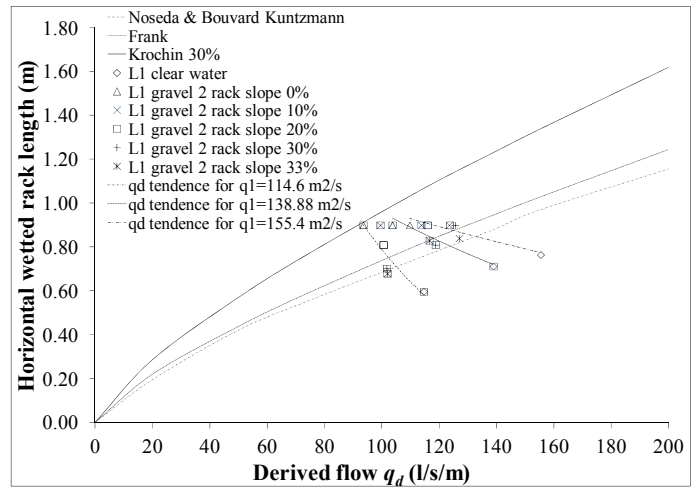


Figure 21. Wetted rack lengths (horizontal projection) for tests carried out with gravel 2, rack C and different flows.

Comparing the wetted rack lengths with research in clear water carried out by Nosedá (1956), Frank (1956), and Bouvard & Kuntzmann (1954), results obtained in laboratory with sediments were longer than the lengths calculated by using their formulae.  $L_l$  tended to have an increment of about 33% of the wetted rack length obtained with clear water. These results match with the values obtained with Krochin formula when 30% occlusion is considered.

At the end of each test, the solids captured by the rack, deposited over it and rejected by the channel were weighted. Figures 22-23 show the rate, in weight, of solids captured by the racks B and C, as a function of the rack slope and the incoming flow. The rate of solids captured increases with the rack slope in the rack B for the smallest incoming flows, and for  $q_l = 114.6$  and  $138.88$  l/s/m in the rack C. However, the behavior of the highest specific flow shows a change in his behavior for slopes steeper than 10% in rack B and 20% in rack C.

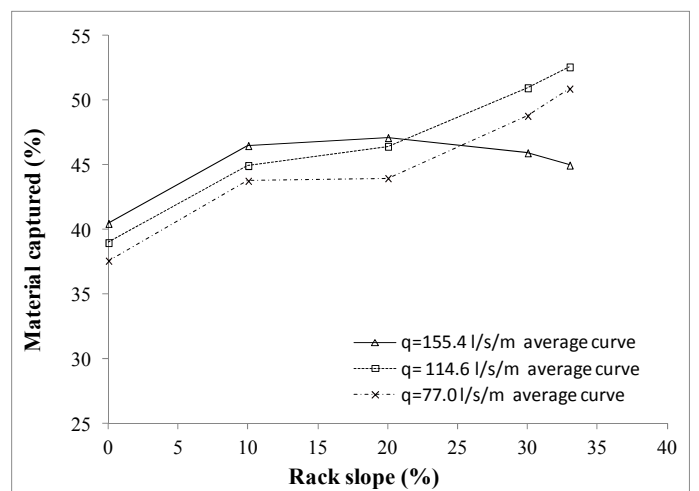


Figure 22. Rate of material collected with rack B and gravel 1.

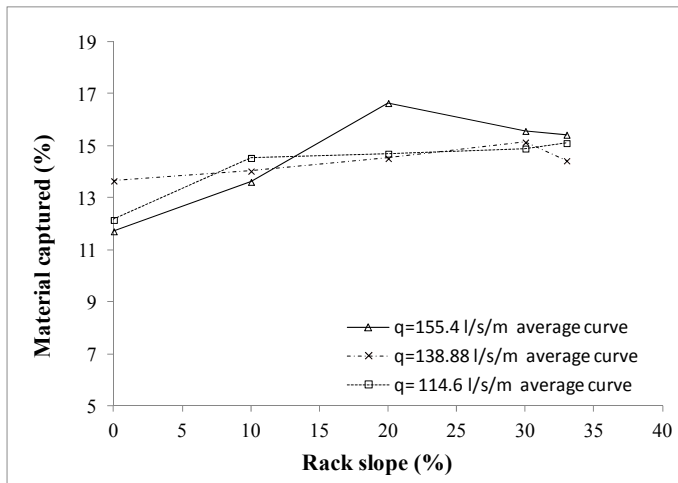


Figure 23. Rate of material collected with rack C and gravel 2.

## 4 CONCLUSIONS

In this work, bottom water intake systems are analyzed in order to utilize them in dry riverbeds. Due to that the rain episodes are torrential in semiarid regions, the objective is to derivate the maximum amount of water with the minimum amount of sediment.

The shape and spacing between bars are parameters that need to be considered as a function of the materials existents in the river bed.

Clear water simulations solved with CFD code obtained a good agreement with experimental data, when several flows and rack slopes where considered.

Sediment experimental tests were focused in the influence of particles whose size was superior to the spacing between bars (the  $d_{50}$  value was equal or superior to the spacing between bars).

Experimental tests showed a decrease of the derived flow due to the effects of occlusion. The decrease is related with the longitudinal rack slope and the maximum efficiency obtained was with a slope of 30%.

The wetted rack lengths obtained with sediments tended to be longer than the obtained with classical formulae.

The flow depths over the bars tended to increase in the experiments with sediments due to the decreasing of the void ratio.

In order to improve the design criteria of intake systems, and their application in ephemeral streams in semiarid regions, it is necessary to do more experimental and numerical studies in both clean water and sediment transport.

## 5 REFERENCES

ANSYS, Inc. (2010). *ANSYS CFX-Solver Theory Guide. Release 13.0.*

- Bouvard, M. 1953. Debit d'une grille par en dessous. *La Houille Blanche* 2: 290-291
- Bouvard, M. & Kuntzmann, J. 1954. Étude théorique des grilles de prises d'eau du type "En dessous". *La Houille Blanche* 5: 569-574
- Bouvard, M. 1992. Mobile Barrages & Intakes on Sediment Transporting Rivers. *IAHR Monograph*. Rotterdam: Balkema.
- Brunella, S., Hager, W. & Minor, H. 2003. Hydraulics of Bottom Rack Intake. *Journal of Hydraulic Engineering*, 129(1): 2-10.
- Castillo, L.G. & Lima, P. 2010. Análisis del dimensionamiento de la longitud de reja en una captación de fondo. *Proc. XXIV Congreso Latinoamericano de Hidráulica, Punta del Este, Uruguay, 21-25 November 2010.*
- Castillo, L. & Carrillo, J.M. 2012. Numerical simulation and validation of intake systems with CFD methodology. *Proc. 2nd IAHR European Congress; Munich, 27-29 June 2012.*
- Castillo, L.G., Carrillo, J.M. & García, J.T. 2013. Comparison of clear water flow and sediment flow through bottom racks using some lab measurements and CFD methodology. *Proc. Seven River Basin Management. Wessex Institute of Technology; New Forest, 22-24 May 2013.*
- Castillo, L.G., Carrillo, J.M. & García, J.T. 2013. Flow and sediment transport through bottom racks. CFD application and verification with experimental measurements. *Proc. 35<sup>th</sup> IAHR Congress, Chengdu, 8-13 September 2013.*
- Castillo, L.G., Carrillo, J.M. & García, J.T. 2013. Comparativa del flujo de agua limpia y con sedimentos a través de sistemas de captación de fondo utilizando datos de laboratorio y un modelo CFD. *Proc. III Jornadas de Ingeniería del Agua, Valencia, 23-24 October 2013*
- Drobir, H. 1981. Entwurf von Wasserfassungen im Hochgebirge. In, *Österreichische Wasserwirtschaft*: 11(12): 243-253.
- Drobir, H., Kienberger, V. & Krouzecky, N. 1999. The wetted rack length of the Tyrolean weir. *Proc. 28<sup>th</sup> IAHR Congress, Graz, 22-27 August 1999.*
- Frank, J. 1959. Fortschritte in der hydraulik des Sohlenrechens. *Der Bauingenieur*, 34: 12-18.
- Frank, J. 1956. Hydraulische Untersuchungen für das Tiroler Wehr. *Der Bauingenieur*, 31(3): 96-101
- Krochin, S. 1978. Diseño Hidráulico. Segunda Edición. *Colección Escuela Politécnica Nacional*. Quito, Ecuador.
- Noseda, G. 1956. Correnti permanenti con portata progressivamente decrescente, defluenti su griglie di fondo. *L'Energia Elettrica*, 565-581.
- Orth, J., Chardonnet, E. & Meynardi, G. 1954. Étude de grilles pour prises d'eau du type. *La Houille Blanche* 3: 343-351.
- Ract-Madoux, M., Bouvard, M., Molbert, J. & Zumstein, J. 1955. Quelques réalisations récentes de prises en-dessous à haute altitude en Savoie. *La Houille Blanche*, 6: 852-878.
- Righetti, M., Rigon, R. & Lanzoni, S. 2000. Indagine sperimentale del deflusso attraverso una griglia di fondo a barre longitudinali. *Proc. XXVII Convegno di Idraulica e Costruzioni Idrauliche*, Genova, 3: 112-119.
- Righetti, M. & Lanzoni, S. 2008. Experimental Study of the Flow Field over Bottom Intake Racks. *Journal of Hydraulic Engineering* 134(1): 15-22.
- Zingg, T. 1935. Beitrag Zur Schotteranalyse, Schweiz. *Mineralog. und Petrog. Mitt., Bd.*, 15: 39-140, 1935.